

# Exploring the Lyman Forest with VLT/UVES

Stefano Cristiani<sup>1,2</sup>, Simone Bianchi<sup>3</sup>, Sandro D’Odorico<sup>3</sup>, Tae-Sun Kim<sup>3</sup>

<sup>1</sup> *ST European Coordinating Facility, K.-Schwarzschild-Str. 2, D-85748 Garching*

<sup>2</sup> *Department of Astronomy, Vicolo dell’Osservatorio 2, I-35122 Padova*

<sup>3</sup> *European Southern Observatory, K.-Schwarzschild-Str. 2, D-85748 Garching*

**Abstract.** A sample of 8 QSOs with  $1.7 < z_{\text{em}} < 3.7$  has been observed with VLT/UVES at a typical resolution 45000 and  $S/N \sim 40 - 50$ . Thanks to the two-arm design of the spectrograph, a remarkable efficiency has been achieved below 400nm and above 800nm, which translates immediately in the possibility of obtaining new results, especially at  $z \lesssim 2.5$ . We report here new insight gained about the evolution of the number density of Ly- $\alpha$  lines, their column density distribution, the ionizing UV background and the cosmic baryon density.

## 1 The number density evolution of Ly- $\alpha$ lines

The swift increase of the number of absorptions (and the average opacity) with increasing redshift is the most impressive property of the Ly- $\alpha$  forest. Fig. 1 shows the number density evolution of the Ly- $\alpha$  lines [8, 9] in the column density interval <sup>1</sup>  $N_{HI} = 10^{13.64-16} \text{ cm}^{-2}$ . The long-dashed line is the maximum-likelihood fit to the data at  $z > 1.5$  with the customary parameterization:  $N(z) = N_0(1+z)^\gamma = (6.5 \pm 3.8)(1+z)^{2.4 \pm 0.2}$ . The UVES [2] observations imply that the turn-off in the evolution does occur at  $z \sim 1$ , not at  $z \sim 2$  as previously suggested. The evolution of the  $N(z)$  is governed by two main factors: the Hubble expansion and the metagalactic UV background (UVB). At high  $z$  both the expansion, which decreases the density and tends to increase the ionization, and the UVB, which is increasing or non-decreasing with decreasing redshift, work in the same direction and cause a steep evolution of the number of lines. At low  $z$ , the UVB starts to decrease with decreasing redshift, due to the reduced number and intensity of the ionizing sources, counteracting the Hubble expansion. As a result the evolution of the number of lines slows down.

Up to date numerical simulations [13] have been remarkably successful in qualitatively reproducing the observed evolution, however they predict the break in the  $dN/dz$  power-law at a redshift  $z \sim 1.8$  that appears too high in the light of the new UVES results. This suggests that the UVB implemented in the simulations may not be the correct one: it was thought that at low redshift QSOs are the main source of ionizing photons, and, since their space density drops below  $z \sim 2$ , so does the UVB. However, galaxies can produce a

---

<sup>1</sup>This range in  $N_{HI}$  has been chosen to allow a comparison with the HST Key-Programme sample at  $z < 1.5$  [15] for which a threshold in equivalent width of  $0.24 \text{ \AA}$  was adopted.

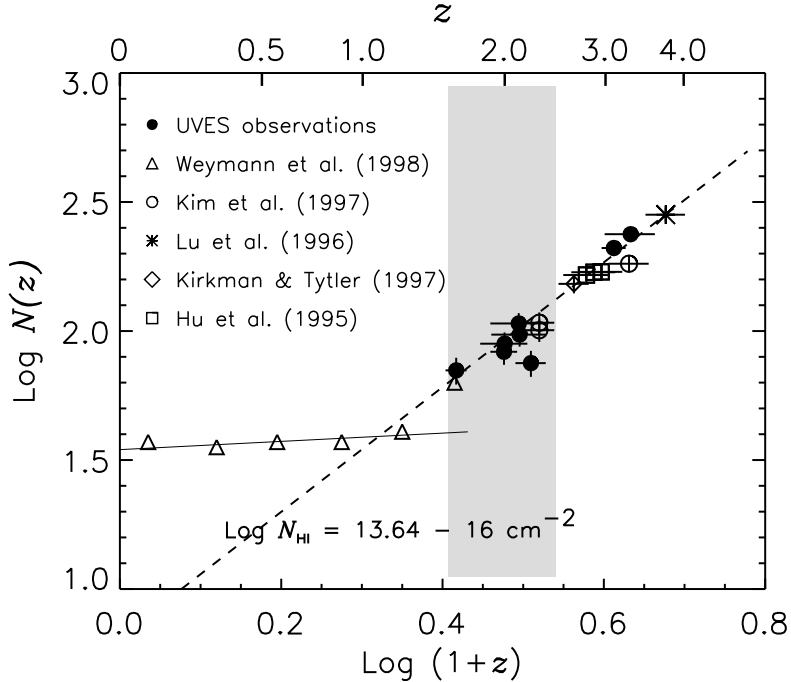


Figure 1: The number density evolution with  $z$  [9]

conspicuous ionizing flux too, perhaps more significant than it was thought[12]. The galaxy contribution can keep the UVB relatively high until at  $z \sim 1$  the global star formation rate in the Universe quickly decreases, determining the qualitative change in the number density of lines. Under relatively general assumptions, it is possible to relate the observed number of lines above a given threshold in column density or equivalent width to the expansion, the UVB, the distribution in column density of the absorbers and the cosmology:

$$\left(\frac{dN}{dz}\right)_{>N_{HI,lim}} = C [(1+z)^5 \Gamma_{HI}^{-1}(z)]^{\beta-1} H^{-1}(z), \quad (1)$$

where  $\Gamma_{HI}$  is the photoionization rate and the  $N_{HI}$  distribution is assumed to follow a power-law of index  $\beta$ , as discussed in the next section.

## 2 The column density distribution

Fig. 2 shows the differential density distribution function measured by UVES [8, 9], that is the number of lines per unit redshift path and per unit  $N_{HI}$  as a function of  $N_{HI}$ . The distribution basically follows a power-law  $f(N_{HI}) \propto N_{HI}^{-1.5}$  extending over 10 orders of magnitude with little, but significant devi-

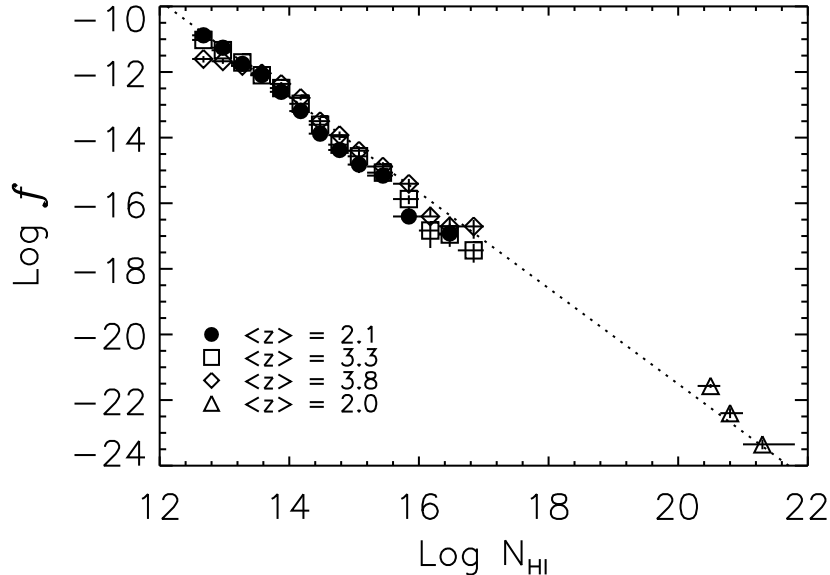


Figure 2: The column density distribution [9]

ations, which become more evident and easy to interpret if the plot is transformed in the mass distribution of the photoionized gas as a function of the density contrast,  $\delta$ , [11]: 1) a flattening at  $\log N_{HI} \lesssim 13.5$  is partly due to line crowding and partly to the turnover of the density distribution below the mean density; 2) a steepening at  $\log N_{HI} \gtrsim 14$ , with a deficiency of lines that becomes more and more evident at lower  $z$ , reflects the fall-off in the density distribution due to the onset of rapid, non-linear collapse: the slope  $\beta$  goes from about  $-1.5$  at  $\langle z \rangle = 3.75$  to  $-1.7$  at  $z < 2.4$  and recent HST STIS data [3] confirm that this trend continues at lower redshift measuring at  $z < 0.3$  a slope of  $-2.0$ ; 3) a flattening at  $N_{HI} \gtrsim 10^{16} \text{ cm}^{-2}$  can be attributed to the flattening of the density distribution at  $\delta \gtrsim 10^2$  due to the virialization of collapsed matter. Hydrodynamical simulations successfully reproduce this behaviour, indicating that the derived matter distribution is indeed consistent with what would be expected from gravitational instability.

### 3 The ionizing background

The last ingredient to be determined in Eq. 1 is the ionization rate. In a recent computation [1] we have investigated the contribution of galaxies to the UVB, exploring three values for the fraction of ionizing photons that can escape the galaxy ISM,  $f_{esc} = 0.05, 0.1$  and  $0.4$  (the latter value corresponds to the Lyman-continuum flux detected by [12] in the composite spectrum of 29 Lyman-break galaxies). Estimates of the UVB based on the proximity effect

at high- $z$  and on the H $\alpha$  emission in high-latitude galactic clouds at low- $z$  provide an upper limit on  $f_{esc} \lesssim 0.1$ , consistent with recent results on individual galaxies both at low- $z$  [4, 7] and at  $z \sim 3$  [5]. Introducing a contribution of galaxies to the UVB, the break in the Ly- $\alpha$   $dN/dz$  can be better reproduced than with a pure QSO contribution [1]. The agreement improves considerably also at  $z \gtrsim 3$ . Besides, models with  $\Omega_\Lambda = 0.7, \Omega_M = 0.3$  describe the flat evolution of the absorbers much better than  $\Omega_M = 1$ .

A consistency check is provided by the evolution of the lower column density lines. For  $\log N_{HI} \lesssim 14$  the  $N_{HI}$  distribution is flatter, and according to Eq. 1 this translates directly into a slower evolutionary rate, which is consistent with the UVES observations[8]:  $dN/dz_{(13.1 < N_{HI} < 14)} \propto (1+z)^{1.2 \pm 0.2}$ . Another diagnostic can be derived from the spectral shape of the UVB and its influence on the intensity ratios of metal lines [10].

## 4 The cosmic baryon density

Given the cosmological scenario, the amount of baryons required to produce the opacity of the Lyman forest can be computed [14] and a lower-bound to the cosmic baryon density derived from the distribution of the Ly- $\alpha$  optical depths. Applying this approach to the effective optical depths measured in the UVES spectra, the estimated lower bound  $\Omega_b \gtrsim 0.010 - 0.016$  is consistent with the BBN value for a low D/H primordial abundance. Most of the baryons reside in the Lyman forest at  $1.5 < z < 4$  with little change in the contribution to  $\Omega$  as a function of  $z$ . Conversely, given the observed opacity, a higher UVB requires a higher  $\Omega_b$ . As pointed out by [6], the large escape fraction measured by [12] would result in an  $\Omega_b \sim 0.06$  in strong conflict either with the D/H or in general with the BBN or with the Ly- $\alpha$  opacity measurements.

## References

- [1] Bianchi S., Cristiani S., Kim. T.-S., 2001, A&A 376, 1
- [2] D’Odorico S., Cristiani S., Dekker H. et al., 2000, SPIE 4005, 121
- [3] Davé R., Tripp T.M., 2001, ApJ 553, 528
- [4] Deharveng J.-M., Buat V., Le Brun V., et al., 2001, A&A 375, 805
- [5] Giallongo E., Cristiani S., Fontana A., D’Odorico S., 2001, in preparation
- [6] Haehnelt M.G., Madau P., Kudritzki R., Haardt F., 2001, ApJ 549, L151
- [7] Heckman T.M., Sembach K.R., Meurer G.R. et al., 2001, ApJ 558, 81
- [8] Kim T.-S., Cristiani S., D’Odorico S., 2001, A&A 373, 757
- [9] Kim T.-S., Carswell R.F., Cristiani S., D’Odorico S., Giallongo E., 2001, MNRAS submitted
- [10] Savaglio S., Cristiani S., D’Odorico S. et al., 1997, A&A 318, 347
- [11] Schaye J., astro-ph/0104272
- [12] Steidel C.C., Pettini M., Adelberger K.L., 2001, ApJ 546, 665
- [13] Theuns T., Leonard A., Efstathiou G., 1998, MNRAS 297, L49
- [14] Weinberg D.H., Miralda-Escudé J., Hernquist L., Katz N., 1997, ApJ 490, 564
- [15] Weymann R.J., Jannuzi B.T., Lu L. et al., 1998, ApJ 506, 1